Structural Eng./Earthquake Eng., JSCE, Vol. 16, No. 1, 45s−54s, 1999 April

REAL TIME CONTROL OF SHAKING TABLE FOR SOIL-STRUCTURE INTERACTION SIMULATION

Kazuo KONAGAI[1], Toyoaki NOGAMI[2], Takeyasu SUZUKI[3]
Tota KATSUKAWA[4] and Atsushi MIKAMI[5]

[1]Member of JSCE, Dr. Eng., Professor, Institute of Industrial Science, University of Tokyo.
(7-22-1 Roppongi, Minato-ku, Tokyo 106-8558, Japan)
[2]Ph. D., Professor, Department of Civil and Environmental Engineering, University of Cincinnati
(Cincinnati, OH 45221, U. S. A.)
[3]Member of JSCE, Dr. Eng., Technical Research & Development Inst., Kumagai Gumi, Co., Ltd.
(Onigakubo, Tsukuba, Ibaragi 300-13, Japan)
[4]Member of JSCE, Technical Research & Development Inst., Kumagai Gumi, Co., Ltd.
(Onigakubo, Tsukuba, Ibaragi 300-13, Japan)
[5]Member of JSCE, Dr. Eng., Research Associate, Institute of Industrial Science, University of Tokyo.
(7-22-1 Roppongi, Minato-ku, Tokyo 106-8558, Japan)

A new method to simulate soil-structure interaction effects in shaking table tests has been presented recently by the authors. In the method, analog circuits or digital signal processors are used to produce soil-foundation interaction motions in real time. Their expressions of interaction motions are based on published rigorous formulations of impulse response functions of foundations on or in layered soils of semi-infinite extents. This paper introduces in its first half a method for simulating soil-structure interaction effects in shaking table tests along with some pieces of equipment contrived for better control of shaking tables. The latter half then describes a simple example of soil-structure interaction simulations.

Key Words : *Dynamic soil-structure interaction, shaking table, model experiment*

1. INTRODUCTION

[1]Such devastating events as the Sounth-Hyogo Earthquake of 1995 seem to have stimulated a sharp rise in the demand for huge shaking tables that allow models weighing more than a thousand tons for example to be tested. Shaking tables are usually driven by servo-hydraulic actuators so that they follow closely input seismic motions. However, a shaking table, when heavily loaded with a structure model to be tested, interacts with the model, and this interaction often causes the table's motion to deviate from the intended time history. Recent advances in adaptive control theory have certainly enhanced the controllability of shaking tables to a great extent[1), 2)], and yet, the motions of a table often have to be adjusted, through iterative trials, to the intended base motions by modifying the input time histories. Generally, the larger a table is, the more difficult it is for the table to be controlled at will.

A large table with improved performance is certainly a necessity in a lot of earthquake-related research. However, faithful reproduction of free-field ground motions on the table may not necessarily be adequate, because actual structures interact with their foundations and the surrounding soils in real earthquakes, causing the ground motions at the structures' bases to deviate from the free-field ground motions. This dynamic interaction is a phenomenon associated with the influx and efflux of energy which is generated by the earthquake excitation and transmitted through the soil-structure interface. It is noted that the difference between the influx and efflux is exactly the energy stored up

[1] This paper is translated into English from the Japanese paper, which originally appeared on J. Struct. Mech. Earthquake Eng., JSCE, No. 598/I-44, pp. 203-210, 1998. 7.

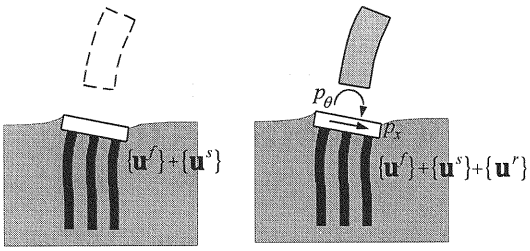

Fig. 1 Seismic soil-structure interaction with sub-structure method

within a structure, and thus, is closely related to the extent of damage to the structure. If these interaction effects are rationally simulated in shaking table tests, one will obtain the necessary pieces of information for interpreting the failure processes of prototype structures in terms of energy.

Konagai and Nogami[4), 5)] have recently developed a method to produce soil-structure interaction effects in a shaking table test on a structure model, without using a physical ground model. In their method, soil-structure interaction effects are simulated by adding appropriate soil-structure interaction motions to the free-field ground motions on the shaking table. Their expressions of soil-structure interaction motions are based on published rigorous formulations of flexibility functions and/or impulse response functions of foundations resting on or embedded in homogeneous or layered soils of semi-infinite extents. In general, radiation damping will cause the total damping of a soil-structure system to be greater than that of the structure itself. Thus, incorporation of soil-structure interaction effects in a shaking table test will lead to a reduction in the demands on the capacity of the table, and the structure model may not necessarily be shaken too forcibly. However, real-time adjustment of the shaking table's motion is definitely a prerequisite for the present method, and one cannot do it through iterative trials.

This paper introduces in its first half a method for simulating soil-structure interaction effects in shaking table tests, in addition to some pieces of equipment contrived for better control of shaking tables. The latter half then describes a simple example of soil-structure interaction simulations using the present method.

2. APPROXIMATION OF SOIL-STRUCTURE INTERACTION MOTIONS

A soil-structure system is divided into two

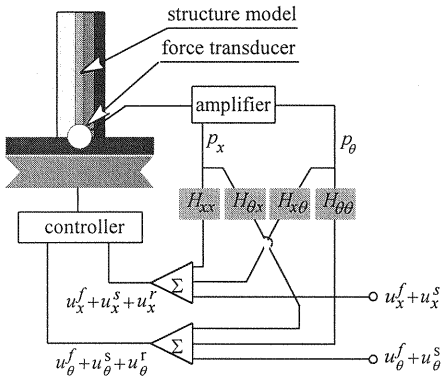

Fig. 2 System for soil-structure interaction simulation

substructures, the super-structure and the unbounded soil extending to infinity; the latter includes an embedded foundation as illustrated in **Fig. 1**. In the lower substructure of soil, an earthquake will cause soil displacements, $\{\mathbf{u}^f\}$. The foundation embedded in this soil deposit, however, will not follow the free-field deformation pattern. This deviation of the displacements from the free-field soil displacements, $\{\mathbf{u}^f\}$, is denoted by $\{\mathbf{u}^s\}$. The mass of the super-structure then causes it to respond dynamically, and the forces, $\{\mathbf{p}\}$, transmitted to the lower substructure of soil and foundation will produce further deformation of soil, $\{\mathbf{u}^r\}$ (***inertia interaction***), that would not occur in a fixed base structure. Thus, the displacements of soil, $\{\mathbf{u}\}$, are eventually expressed by the following equation as:

$$\{\mathbf{u}\}=\{\mathbf{u}^f\}+\{\mathbf{u}^s\}+\{\mathbf{u}^r\} \tag{1}$$

Consider the case that a foundation has two degrees of freedom in sway and rocking (x, θ) at the base of its super-structure as illustrated in **Fig. 1**. The interaction forces, $\{\mathbf{p}\}$ ($=\{p_x \quad p_\theta\}^T$), from the super-structure cause the inertia interaction motions, $\{\mathbf{u}^r\}$, in the frequency domain to be:

$$\begin{Bmatrix} u_x^r \\ u_\theta^r \end{Bmatrix}=\begin{bmatrix} H_{xx}(s) & H_{x\theta}(s) \\ H_{\theta x}(s) & H_{\theta\theta}(s) \end{bmatrix}\begin{Bmatrix} p_x \\ p_\theta \end{Bmatrix} \tag{2}$$

where,

$$\begin{bmatrix} H_{xx}(s) & H_{x\theta}(s) \\ H_{\theta x}(s) & H_{\theta\theta}(s) \end{bmatrix}=[\mathbf{H}] \tag{3a}$$

is the flexibility (compliance) at the top of the foundation, and

$$s=i\cdot\omega \tag{3b},$$

in which $i=\sqrt{-1}$ and ω is the excitement circular frequency. In the present method, a shaking table's

motion is controlled directly following the above-mentioned process of soil-structure interaction. **Fig. 2** shows a schematic view of the set-up in a shaking table test for earthquake simulation, in which a superstructure model is placed directly on the table without a physical ground model. The soil-structure interaction effects are simulated by adding appropriate soil-structure interaction motions to the free-field ground motions at the shaking table. In the simulation, first, the transducers at the base of the foundation pick up the signals of the base forces, p_x and p_θ in sway and rocking motions, respectively. These two amplified signals are then applied to the circuits H_{xx}, $H_{\theta x}$, $H_{x\theta}$ and $H_{\theta\theta}$ to produce the outputs corresponding to the soil-structure interaction motions, u_x^r and u_θ^r. The output signals are then added to the signals of the base input motions, $u_x^f + u_x^s$ and $u_\theta^f + u_\theta^s$, to produce the signals of foundation motions, $u_x^f + u_x^s + u_x^r$ and $u_\theta^f + u_\theta^s + u_\theta^r$. The method is, thus, based on the premise that $u_x^f + u_x^s$ and $u_\theta^f + u_\theta^s$ are known beforehand as the base input motions. The signals of the foundation motions are finally translated into the shaking table motions by the shaking table controller.

This method, therefore, requires a device that can generate signals identical to the transient motion of its base on a soil medium of infinite extent. Rigorous and approximate expressions of unit-impulse response functions for lateral, vertical and rotational vibration modes of a foundation have been presented by a number of researchers (Meek and Wolf[3), 4)], Nogami and Konagai[5), 6)]). Reviewing these expressions, Konagai and Nogami[5), 6)] showed that they are closely approximated by summing up exponential and/or exponentially decaying sine and cosine functions of time *t*, the functions being easily produced by simple analog circuits and/or digital signal processors, namely,

$$h(t) = \sum_0^n A_j h_j(t) \tag{4}$$

where, A_j are unknown constants, and

$$h_j(t) = e^{-\alpha_j t}\cos(\omega_j t - \phi_j) \tag{5}$$

with α_j^{-1} = time constant, ω_j = circular frequency that can be zero, and ϕ_j = phase lag. Applying the Laplace transform to equation (5) leads to:

$$H_j(s) = \frac{(s+\alpha_j)\cdot\cos\phi_j + \omega_j\cdot\sin\phi_j}{(s+\alpha_j)^2 + \omega_j^2} \tag{6}$$

From equation (6), it is found that the Laplace transform of equation (4) eventually has a rational

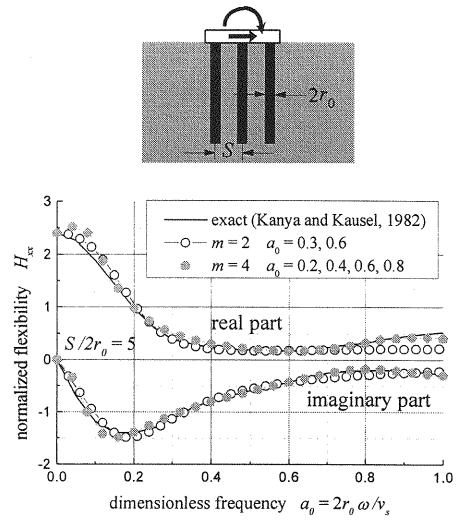

Fig. 3 Dynamic flexibility of 3×3 pile group for harmonic loading

form that is described as:

$$H(s) = \frac{a_m s^m + a_{m-1}s^{m-1} + \cdots + a_1 s + H(0)}{b_m s^m + b_{m-1}s^{m-1} + \cdots + b_1 s + 1} \tag{7}$$

where, a_j and b_j ($j = 1, 2, \cdots, m$) are unknown constants, and $m \le 2n$. The constant, a_m, must be zero as far as the Laplace transforms, $H_j(s)$, (equation (6)) for different values of j are added up. However, the constant, a_m, is intentionally left in equation (7) for a more general expansion of the present method. Equation (7) is rewritten as:

$$\{\mathbf{S}\}\{\mathbf{a}\} = H(0) - H(s) \tag{8}$$

where,

$$\{\mathbf{S}\} = \{-s^m \quad \cdots \quad -s \quad s^m H(s) \quad \cdots \quad sH(s)\}, \tag{9a}$$

and

$$\{\mathbf{a}\} = \{a_m \quad \cdots \quad a_1 \quad b_m \quad \cdots \quad b_1\}^T \tag{9b}$$

The $2m$ unknown constants included in the coefficient vector $\{\mathbf{a}\}$ are determined in such a way that $\{\mathbf{a}\}$ allows the approximate expression of $H(s)$ described in equation (7) to best-fit its rigorous values in a desired frequency range. Since equation (8) should be satisfied for both its real and imaginary parts, m values of s are first taken within this frequency range. Then, m pairs of equation (8) (real and imaginary parts) at these particular points of s eventually make up a set of $2m$ simultaneous equations, and solving the linear simultaneous equations, one obtains all the coefficients in $\{\mathbf{a}\}$.

It will be worthwhile examining how closely the expression in equation (7) approximates rigorous

solutions of flexibilities. **Fig. 3** shows the variation of flexibility, H_{xx}, at the cap of a 3×3 pile group (Kanya and Kausel[7]) with respect to the dimensionless frequency, a_0 $(=2r_0\omega/v_s = 2r_0 s/iv_s)$. The parameters, r_0 and v_s, are the radius of pile and the shear wave velocity in the surrounding soil, respectively. There are two numerical examples of simulation shown in this figure; one with the number of unknown constants $2m$ set at 4 ($a_0 = 0.3$ and 0.6), another with $2m = 8$ ($a_0 = 0.2$, 0.4, 0.6 and 0.8). The larger the number of coefficients is, the more closely the approximate expression fits the rigorous values. It is, however, noted in this figure that even a small number of coefficients ($2m = 4$) eventually allow the close approximation to be realized over almost the entire extent of the frequency range ($0 \le a_0 \le 1$) in this figure. The number of coefficients for approximation should be reduced to some allowable minimum. Meek and Wolf[3), 4)] have developed approximate expressions of flexibility functions for vertical, sway and rocking motions of a rigid mat foundation (radius $=r_0$) on a homogeneous half-space. Their expressions are interpreted in such a way that the allowable minimum of the number of coefficients is eight ($2m = 8$) in order for a close approximation to be obtained within the frequency range, $0 \le a_0 \le 5$. As for an embedded rigid foundation, Konagai and Nogami[5), 6)] have demonstrated that the same number of coefficients allow the flexibility function to be closely approximated for its rocking motion within the same frequency range.

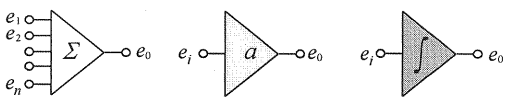

(a) adder **(b)** linear amplifier **(c)** integrator

Fig. 4 Key circuits

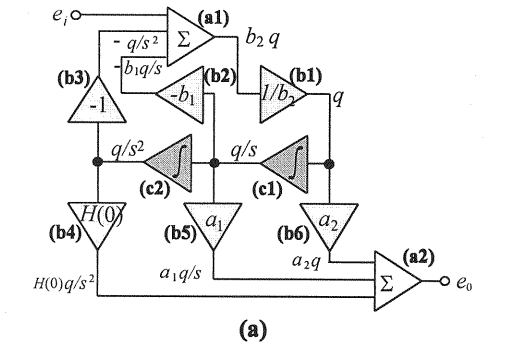

(a)

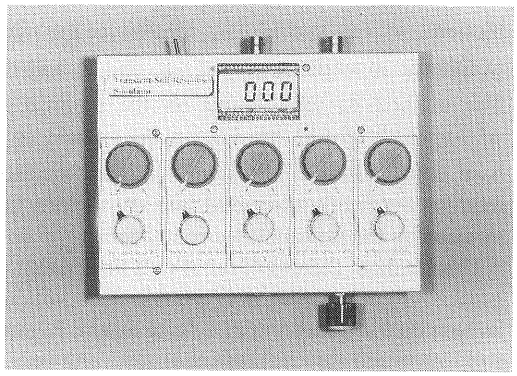

(b)

Fig. 5 Analog circuit to generate

3. PRESENT SYSTEM

(1) Equivalent analog circuits

Electric signals can be controlled by using analog circuits. The first-level units in the circuits are operational amplifiers and passive elements (resisters and capacitors).[8)] These units form an adder (**Fig. 4a**), an amplifier (**Fig. 4b**) and an integrator (**Fig. 4c**) which add several different input signals ($e_1, e_2, \cdots e_n$) together, multiply an input signal, e_i, by a scale factor, a, and integrate a signal, e_i, respectively. The functions of both the adder and the amplifier can actually be realized by one sole circuit called a "scaled adder". For the sake of simple explanations, however, they are separately shown in **Figs. 4a** and **4b**.

Setting the number m at 2 in equation (7), for example, the input and output signals, e_i and e_o, of the circuit for producing the interaction motion u^r should satisfy:

$$H(s) = \frac{a_0 + a_1 s + a_2 s^2}{b_0 + b_1 s + b_2 s^2} = \frac{e_o}{e_i} \qquad (10)$$

Introducing an unknown quantity q, the above equation (19) can be separated into the following two equations as:

$$e_o = a_0 \frac{q}{s^2} + a_1 \frac{q}{s} + a_2 q \qquad (11a)$$

$$e_i = b_0 \frac{q}{s^2} + b_1 \frac{q}{s} + b_2 q \qquad (11b)$$

With the expression in equations (11a) and (11b), the circuit that is capable of generating e_o to an arbitrary input signal e_i is designed as shown in **Fig. 5a**. The input signal e_i and two additional signals, which will be shown later identical to $-q/s^2$ and $-b_1 \cdot q/s$,

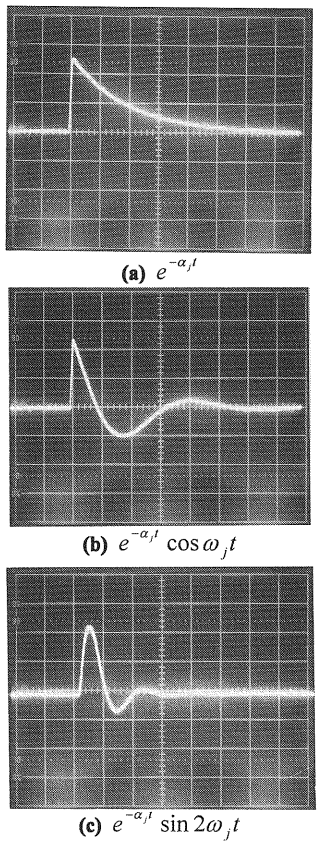

(a) $e^{-\alpha_j t}$

(b) $e^{-\alpha_j t}\cos\omega_j t$

(c) $e^{-\alpha_j t}\sin 2\omega_j t$

Fig. 6 Basic response functions generated by the present analog circuit (0.1 s/div.)

are added together first by the adder **(a1)** and then multiplied by $1/b_2$ by the linear amplifier **(b1)**. The output signal in the above process is q according to equation (11b). Noting that integrating a signal is equivalent, in the frequency domain, to dividing its Fourier spectrum by s, integrators **(c1)** and **(c2)** produce signals q/s and q/s^2, respectively. After these two signals go through linear amplifiers **(b2)** and **(b3)** with scale factors $-b_1$ and -1 respectively, they become $-b_1 \cdot q/s$ and $-q/s^2$, and return to the adder **(a1)**: whereas linear amplifiers **(b4)**, **(b5)** and **(b6)** produce $H(0)\cdot q/s^2$, $a_1 q/s$ and $a_2 q$ respectively, which are added together by the adder **(a2)**. It is now clear from equation (11a) that the output of the adder **(a2)** is identical to the signal e_o.

Fig. 5b shows a model for a test try of **Fig. 5a**-equivalent circuit. Five pairs of knobs are for tuning the five scale factors in **Fig. 5a**. In **Figs. 6a-6c** examples are shown for the transient response of the circuit ($\alpha_j = 5.5\ \mathrm{s}^{-1}$, $\omega_j = 15.7\ \mathrm{s}^{-1}$) to an impulse (rectangular pulse of 5V, duration time = 10 ms).

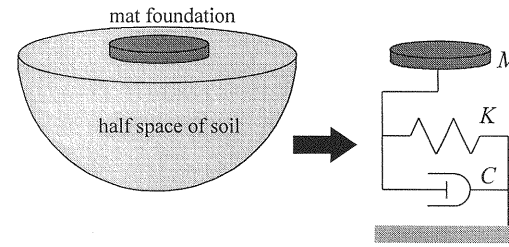

Fig. 7 Equivalent spring-damper system supporting a rigid mat foundation

Only tuning the parameters to prescribed values allows any of the basic response functions to be generated.

(2) Controller of shaking table

It is noted that the system illustrated in **Fig. 2** is realized on condition that a shaking table loses no time in producing faithfully its input motion, $\{\mathbf{u}\}$ $(=\{\mathbf{u}^f\}+\{\mathbf{u}^s\}+\{\mathbf{u}^r\})$. The motion produced by the shaking table, however, is not exactly identical to the intended time history because the ratio of output-to-input amplitude of the shaking table system does not remain the same over the desired frequency range. The performance of the system's transfer function is also affected by the presence of models on the shaking table; this fact may cause the motion of the table to further deviate from the intended time history. A controller with the transfer function T normally performs like a low pass filter, and experiments on the table are conducted below its cut-off frequency. Below this frequency yet, there remains a time delay Δt between the produced motion and the input signal. The effect of the time delay, described in the frequency domain as $T \cong e^{-i\omega\Delta t}$, could be canceled by multiplying the flexibility function H by T^{-1}. Assuming that the performance of a soil-foundation system is approximated by that of a simple-damped oscillator with a spring K, a dashpot C and a mass M (**Fig. 6**), the flexibility function H_{xx} is expressed as:

$$H_{xx} = \frac{1}{K - \omega^2 M + i\omega C} \tag{12}$$

Thus, the cancellation of the time-delay effects is made by

$$H_{xx}T^{-1} \cong \frac{e^{i\omega\Delta t}}{K - \omega^2 M + i\omega C} \tag{13a}$$

For smaller values of $\omega\Delta t$, equation (13a) is rewritten as:

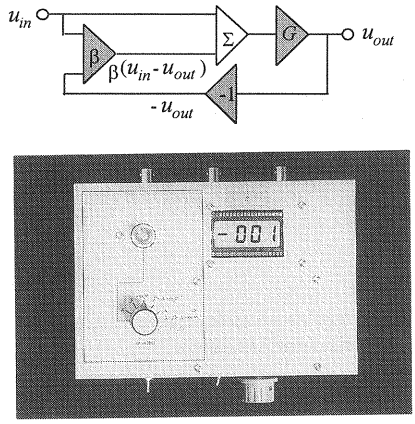

Fig. 8 Servo-amplifier

$$H_{xx}T^{-1} \cong \frac{1}{K-\omega^2(M-\Delta M)+i\omega(C-\Delta C)} \quad (13b)$$

where,

$$\Delta M = C\cdot\Delta t \quad (14a)$$

$$\Delta C = K\cdot\Delta t \quad (14b)$$

Equation (13b) shows that the equivalent mass and the viscous damping coefficient are reduced by $C\Delta t$ and $K\cdot\Delta t$, respectively. The reduced mass $M-\Delta M$ and the damping coefficient $C-\Delta C$ must be positive, calling for:

$$\frac{\Delta M}{M} = 4\pi^2\frac{t_c\Delta t}{t_0^{\,2}} < 1 \quad (15a)$$

$$\frac{\Delta C}{C} = \frac{\Delta t}{t_c} < 1 \quad (15b)$$

with

$$t_c = C/K \quad (16a)$$

$$t_0 = 2\pi\sqrt{M/K} \quad (16b)$$

The above conditions (equations (15a) and (15b)) are usually satisfied in reality for many cases of soil-structure interaction, because radiation of waves from a foundation leads the motion of the structure to be noticeably damped.

It is, however, necessary for the time delay to be minimized when equations (15a) and (15b) are not satisfied. One possible measure for reducing the time delay is to increase the feedback gain of a servo-amplifier of the shaking table (**Fig. 8**). In **Fig. 8**, u_{in} and u_{out} are the input signal and the signal of the motion produced by the shaking table, respectively. The deviation of the produced motion from the input signal, $u_{out}-u_{in}$, is multiplied by a negative factor $-\beta$, and is added to the input signal u_{in}. The following relationship between u_{in} and u_{out} is then satisfied with the original transfer function of the controller itself ($\beta=0$) denoted by G:

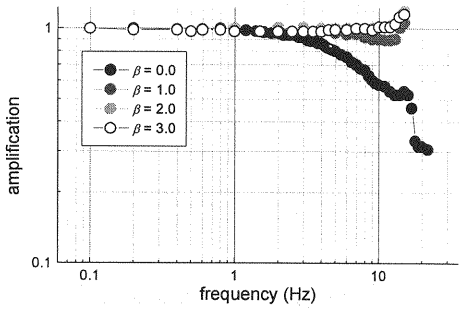

(a) phase lag

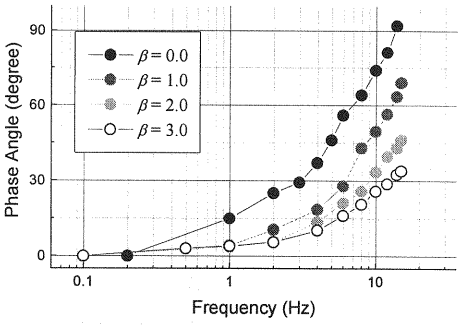

(b) amplitude

Fig. 9 Effect of feed-back gain on shaking-table transfer function

$$u_{out} = G(u_{in} + \beta(u_{in} - u_{out})) \quad (17)$$

From equation (17), the overall transfer function T is described as:

$$T = \frac{u_{out}}{u_{in}} = \frac{G+G\beta}{1+G\beta} \quad (18)$$

It is noted in equation (18) that T comes closer to 1 as the feedback gain, β, increases. The servo-amplifier shown in **Fig. 8** was built in a one-dimensional shaking table system to check its performance. **Fig. 9** shows that a servo-amplifier with a larger value of β offers more significant improvement in expanding the frequency range in which the ratio of output-to-input amplitude remains almost constant with little phase-shift. The increase of β, however, leads to a decrease in the margin for unstable clattering of the table that is caused by the noise echoing through the closed circuit of the servo-amplifier.

4. EXPERIMENT

In order to provide a proper perspective on the usefulness of the present method, a simple example

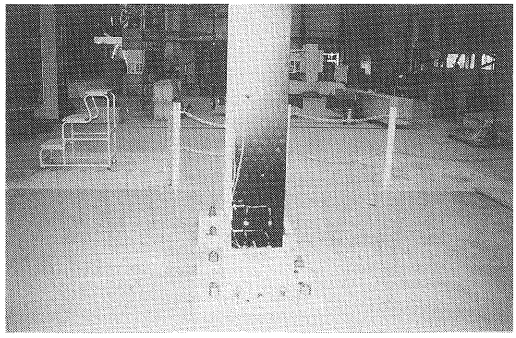

Fig. 10 Upright beam on shaking table

Table 1 Parameters of cantilever

width (m)	height (m)	thickness (m)	Bending stiffness EI (Nm^2)	density ρ (kg/cm^3)
0.3	1.8	0.008	2132.5	0.00801

Table 2 Soil properties

Density ρ_s (kg/cm^3)	shear wave velocity v_s (m/s)	Poisson's ratio ν
0.0016	4.8	0.5

Table 3 Parameters for foundation

Radius r_0 (m)	thickness d (m)	density ρ_c (kg/cm^3)
0.8	0.1	0.0025

of simulation of soil-structure interaction effects is introduced herein. Eight steel plates (2000 mm × 300mm × 1 mm) were fastened together with rivets arranged in a grid to form a simple cantilever. The cantilever was then fixed upright on a shaking table with six degrees of freedom, as shown in **Fig. 10**[9], because it was expected that the bending of the cantilever would cause a rocking motion in its foundation. The feedback gains, β, of the servo-amplifier for this shaking table are set at 0.53 and 0.41 in respect to horizontal and rocking degrees of freedom. Mechanical properties of the cantilever are listed in **Table 1**. The cantilever is rather flexible, with its natural frequency set approximately at 1Hz, so that interaction forces (both shear force p_x and moment p_θ) are easily measured by bonding strain gages to the lower end of the cantilever. This flexible cantilever was assumed to be mounted virtually on a circular rigid mat foundation (radius (r_0) = 1.2 m, thickness (d) = 0.2 m, **Table 3**) resting on a soft semi-infinite half-space of soil (v_s = 9 m/s, **Table 2**). Meek and Wolf[3), 4)] have developed a unified approach for soil-structure interaction analysis by using truncated semi-infinite cone models

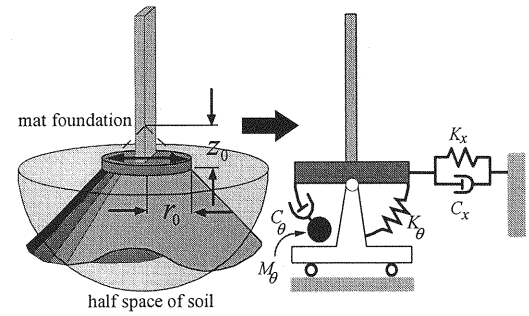

Fig. 11 Mat foundation and equivalent discrete element model

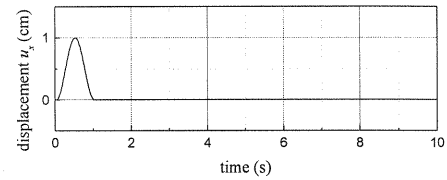

Fig. 12 Input base motion $u_x^f + u_x^s$

representing an unbounded soil medium. According to their approach, the soil supporting a rigid mat foundation is idealized for each degree of freedom as a truncated semi-infinite elastic cone with its own apex height z_0 (**Fig. 11**). They also showed that the stiffness parameters for sway and rocking motions are approximated by those of discrete element models illustrated in **Fig. 11**. The flexibility, $H_{xx}(s)$, of the discrete-element model in horizontal x direction is described as:

$$H_{xx}(s) = \frac{1}{sC_x + K_x} \tag{19}$$

where,

$$K_x = \frac{\rho_s v_s^2 \cdot \pi r_0^2}{z_0} \tag{20a}$$

$$C_x = \rho_s v_s \cdot \pi r_0^2 \tag{20b}$$

and v_s is the shear wave velocity propagating through the cone that dominates the stiffness within considerably high frequency range. The apex ratio z_0 / r_0, or the opening angle of the cone, is determined by simply equating the static stiffness coefficient of the disk on the semi-infinite soil half-space to that of the corresponding cone, and is given by:

$$\frac{z_0}{r_0} = \frac{\pi}{8}(2-\nu) \tag{20c}$$

As far as the rocking motion of the disk is concerned, a rotational cone should be discussed. The flexibility, $H_{\theta\theta}(s)$, of the equivalent-discrete-element model in rocking motion is described as:

$$H_{\theta\theta}(s) = \frac{\frac{1}{C_\theta}s + \frac{1}{M_\theta}}{s^2 + \frac{K_\theta}{C_\theta}s + \frac{K_\theta}{M_\theta}} \tag{21}$$

where,

$$K_\theta = \frac{3\rho_s v^2 I_0}{z_0} \tag{22a}$$

$$C_\theta = \rho_s v I_0 \tag{22b}$$

$$M_\theta = \rho_s z_0 I_0 \tag{22c}$$

with $$I_0 = (\pi/4) r_0^4 \tag{22d}$$

The velocity v is assumed to be identical to that of the longitudinal wave traveling through the cone when Poisson's ratio of the soil is less than 1/3. For larger values of Poisson's ratio, v is set at $2v_s$. The apex ratio z_0 / r_0 of the rotational cone is:

$$\frac{z_0}{r_0} = \frac{9\pi}{32}(1-\nu)\left(\frac{\nu}{v_s}\right)^2 \tag{22e}$$

In actuality, the lateral and rocking motions of a foundation are coupled, and the present method illustrated in **Fig. 2** allows the effect of the coupling to be simulated. The coupling effect, however, is ignored in this simulation. Equations (19) and (20) indicate that the present example is described by equation (7) with *m* set at 2.

As has been mentioned, electric-resistance strain gages were used as a sensing device for both shear-force and moment. A pair of strain gages were bonded on both sides of the lower end of the cantilever to sense the strain in the cantilever resulting from the bending motion of the cantilever. The outputs of strain gages are then connected to an appropriate bridge circuit that produces a signal proportional to the bending moment. Another pair of strain gages were then pasted 10 cm above them, and the measurement of moments at these two points permitted a determination of the shear force at the lower end of the cantilever. It is noted that the moment and the shear force sensed by these strain gages are not identical yet to the interaction forces, p_x and p_θ, on the soil-foundation interface. The interaction forces are to be evaluated taking into account the inertia forces of the foundation virtually resting on the half-space of soil. For this evaluation,

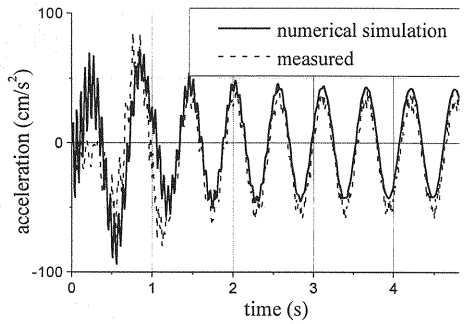

(a) without interaction

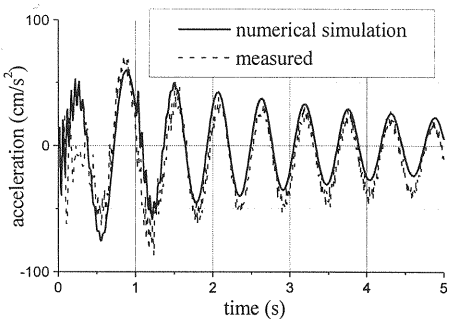

(b) with interaction

Fig. 13 Accerelation at the top end of upright beam

both lateral and rocking accelerations, $\ddot{u}_x$ and $\ddot{u}_\theta$, were measured on the shaking table, and the signals of $\ddot{u}_x$ and $\ddot{u}_\theta$ were multiplied respectively by the foundation mass, M_x $(=\rho_c \cdot \pi \quad r_0^2 d)$, and the moment of inertia, M_p $(=\rho_c I_0 d + M_{trap})$, where M_{trap} is the contribution of the soil mass caught beneath the foundation, and is given by:

$$M_{trap} = 1.2\left(\nu - \frac{1}{3}\right)\rho_s I_0 r_0 \tag{23}$$

A horizontal impulse shown in **Fig. 12** was given to the shaking table as an effective foundation input motion, $u_x^f + u_x^s$, and the acceleration response at the top end of the cantilever was measured. The dotted line in **Fig. 13a** shows the acceleration time history without the interaction motions, u_x^r and u_θ^r, being added; whereas the dotted line in **Fig. 13b** shows the response affected by the interaction motions. Thick lines in these figures show the

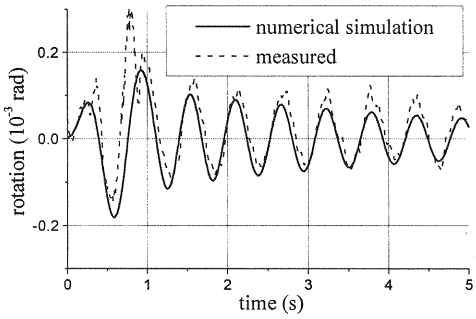

Fig. 14 Rocking of shaking table

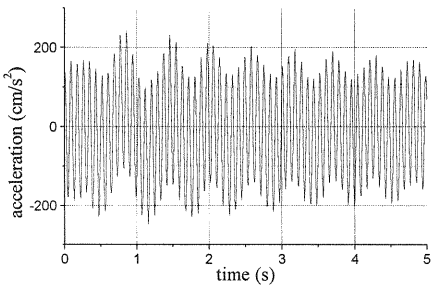

Fig. 15 Howling observed at the top end of upright beam

computed responses of the discrete element model in **Fig. 11**. In this numerical simulation, the finite difference method was utilized to obtain the solutions in the time domain. The thick and dotted lines are in good agreement in both figures; this fact clearly demonstrates that, for the simulation of soil-structure interaction motions, the present method works properly as expected. These figures show that incorporating the effect of the interaction motion leads to the increase of damping and to the slight decrease of natural frequency as well. Although only horizontal base motion was given to the shaking table, bending motion of the cantilever eventually caused the shaking table (the virtual foundation) to rock as shown in **Fig. 14**. The observed rocking motion, u_θ^r, is also in good agreement with the numerical simulation (thick line).

The present system is conditionally stable as is often the case with feed-back control systems. Especially when a structure model with low damping ratio is shaken, the motion of the shaking table sometimes echoes through the circuit causing a serious clattering (howling) of the table. **Fig. 15** shows one example of clattering that happened before the table was properly heated up and stabilized. The predominant frequency of the noise is 11 Hz, and is about identical to the fourth natural circular frequency of the model. When the predominant frequency is higher than the frequency range in which the desired signal exists, a low-pass filter may be used to reduce the noise. It is however noted that the use of a low-pass filter causes the response of the table to be more delayed. Some built-in device such as an adaptive echo canceller[10] would be useful for further improving its performance. Detailed study on this improvement will be addressed in a later publication.

5. CONCLUSIONS

A new method for a model experiment on a shaking table has been presented. The present method allows soil-structure interaction to be simulated. The conclusions of this study are summarized as follows:

(1) In the present method, soil-structure interaction effects are simulated by adding appropriate soil-structure interaction motions to the free-field ground motions at the shaking table. A variety of unit-impulse response functions of bases or soil mediums overlaid with structures are closely approximated by summing up basic functions which can be generated by simple analog circuits and/or digital signal processors. This method thus has the potential to be applied to a variety of experiments of soil-structure interaction without preparing any physical soil model.

(2) The present system is realized on condition that a shaking table produces faithfully its input motion. The motion produced by the shaking table, however, is not exactly identical to the intended time history because the ratio of output-to-input amplitude of the system does not remain the same over the frequency range desired. The performance of the system's transfer function is also affected by the presence of a model on the shaking table, a fact that may cause the motion of the table to further deviate from the input. This effect will be canceled by multiplying the flexibility function, H, of a soil-foundation system by the inverse transfer function, T^{-1}, of the shaking table system. This manipulation, however, leads to reducing both the mass, M, and the viscous damping coefficient, C, making up the discrete element model equivalent in mechanical properties to the soil-foundation system. Needless to say, the reduced mass, $M-\Delta M$, and the damping coefficient, $C-\Delta C$, must be positive. The conditions are

usually satisfied in reality for many cases of soil-structure interaction because wave radiation from a foundation leads the motion of the structure to be noticeably damped. If not, it would be necessary for the time delay to be minimized. One possible measure for reducing the time delay is to increase the feedback gain of a servo-amplifier of the shaking table. It is, however, noted that the increase of feedback gain leads to a decrease in the margin for unstable clattering of the table that is caused by the noise echoing through the closed circuit of the servo-amplifier.

(3) In order to provide a proper perspective on the usefulness of the present method, a simple upright 2,000 mm long steel cantilever was shaken on a shaking table. The observed responses of the beam showed that incorporating the effect of the interaction motion leads to the increase of damping and to the slight decrease of natural frequency as well. The numerical simulations were in good agreement with the observed responses, demonstrating that the present method for the simulation of soil-structure interaction motions works properly as expected. It is, however, noted that unexpected noise amplification can cause serious problem in operating the shaking table when a less-damped structure model is tested on a shaking table.

ACKNOWLEDGMENT: Partial financial support for this study has been provided by the Ministry of Education, Science and Culture (Grants-in-Aid for Scientific Research, No. 09875109 and No. 10450174). The authors are indebted to Mr. Toshihiko Katagiri, IIS, Univ. of Tokyo, and Mr. Osamu Uemura, Japan Highway Public Corporation, (formerly a graduate student, Univ. of Tokyo), for their help throughout the experiments.

REFERENCES

1) Horiuchi, T., Nakagawa, M., Sugano, M., and Konno, T.: Development of Real-Time Hybrid Experiments System with Actuator Delay Compensation, *Jour., JSME* (C), **61(584)**, 64-72, 1995 (in Japanese).
2) Stoten, D.P. and Gomez, E: Recent Application: Results of Adaptive Control on Multi-Axis Shaking Tables, *Proc., 6th SECED Int. Conf., Seismic Design Practice into the Next Century*, Booth (ed.), 381-387, 1998.
3) Meek, J. W. and Wolf, J. P.: Cone models for homogeneous soil, *J. geotechnical eng., ASCE*, **118(5)**, pp. 667-685. 1992.
4) Meek, J. W. and Wolf, J. P.: Cone models for embedded foundation, *J. geotechnical eng., ASCE*, **120(1)**, pp. 60-80, 1992.
5) Konagai, K. and T. Nogami: Simulation of Soil-Structure Interaction on a Shaking Table, "Numerical and Physical Modeling for Dynamic Soil/Structure Interaction Phenomenon", *Geotechnical Special Technical Publication, ASCE*, **64**, pp. 91-106, 1997.
6) Konagai, K. and T. Nogami: Analog Circuits for Simulating Soil-Structure Interaction on a Shaking Table, *Intrn. Jour., Soil Dynamics and Earthquake Engineering*, accepted for publication, 1997.
7) Kanya, A. M. and E. Kauzel, Dynamic Behavior of Pile Groups, *Proc., 2nd International Conference on Numerical Methods of Offshore Piling*, Austin, TX, pp. 509-532, 1982.
8) Zadeh, L. A. and C. A. Desoer: *Linear System Theory*, McGraw-Hill Book Co., 1963.
9) Konagai, K. and Katsukawa, T.: Real time control of a shaking table for soil-flexible structure interaction, *Bull., Earthquake Resistant Structure Research Center*, IIS, Univ. of Tokyo, **30**, pp. , 1997.
10) Sondhi, M. M.: An Adaptive Echo Canceller, Bell Syst. Tech. Jour., 46(3), p.497, 1967.